Kinetic and Mechanism of Oxidation of Hydrogen Sulfide Over Fe/SiO$_2$ Catalyst

HOSSEIN ATASHI*, MEHDI SAHEBI-SHAHEMABADI, ARASH ARA and BAHMAN SHIRZADI
Department of Chemical Engineering, University of Sistan & Baluchestan,
Zahedan, P.O. Box-98165-161, Iran
Tel: (98)(912)1193366; E-mail: h.ateshy@hamoon.usb.ac.ir

The hydrogen sulfide oxidation kinetics for sulphur production over Fe/SiO$_2$ catalyst was studied in a cylindrical fixed bed reactor at 0.9 atmospheric pressure and 200-270 ℃ temperature range was used. Results show that hydrogen sulfide reacts over catalyst through two separately pathway. It is believed that the sulphur formation from hydrogen sulfide, take place in a reversible pathway. Kinetic conclusion and subsequently the reaction mechanism, was performed upon experimental measurements of reaction product concentration values.

Key Words: Kinetic, Mechanism, Hydrogen sulfide oxidation, Catalytic oxidation.

INTRODUCTION

In the gas refineries and petrochemical complexes, first, the H$_2$S separated from natural gas in the amine unit, because of equipment corrosion, catalyst deactivation and other problems that occurs in the presence of H$_2$S gas. For many years, most of the hydrogen sulphide (from natural gases or oil field) is transformed into harmless sulphur using the Claus process[1,2]. The complete transformation of H$_2$S can be achieved using several processes[3,4]. For treating low concentration (less than 5 vol. %) of sulphur-containing gas in the tail gas from the Claus plant or other emission source, various commercial processes have been used that are based on adsorption, absorption and wet oxidation[5,6].

The dry catalytic processes were based on the selective catalytic oxidation of H$_2$S to elemental sulphur. Many catalysts have been studied for this reaction. Examples of commercially developed catalysts for the processes are the titanium-based catalysts that is used in MODOP processes[7,8] and the iron-based catalysts in Super-Claus process[9-16].

However, the Super-Claus process cannot treat high concentration of H$_2$S above 2 vol. % because it is necessary to supply excess oxygen (usually 10 times the stoichiometric amount) to overcome catalytic deactivation caused by the water[17-19].

Various binary oxides such as V-Mg, V-Bi, V-Mo, V-Sb and Fe-Sn, Bi-Mo were tested without feeding water in excess oxygen[20,21]. Recently, the activity of iron-based multi-metallic oxides was reported through patents[18,22].

Actually, iron oxide is highly efficient for H_2S oxidation, but scarcely selective. The Van den Brink researches represented that if we use the ferric sulfate catalyst, which distributed on the silica basis in the finely powder form, the catalyst selectivity and the amount of sulphur production will be excellent. Novak and Zdrazil were used $Fe_2O_3/\alpha\text{-}Al_2O_3$ catalyst in their works. Their results show that the sulphur production in the catalyst, which contains greater pores, is greater. It was not provided the conversion rate equation of H_2S and just noted the temperature, pressure and H_2S inlet concentration limits.

In the present study, the catalytic oxidation kinetic of H_2S was studied and a suitable rate relationship was provided, also an appropriate mechanism was suggested for H_2S oxidation with air, at the catalyst adjacent, accompanying optimized condition of sulphur production.

EXPERIMENTAL

The kinetic experiments were performed in a cylindrical fixed bed reactor with stainless still (TYPE 316), internal diameter of 24.9 mm and external diameter of 36 mm. Procatalyst CT-739[R] with 4 mm diameter packed the reactor. Catalyst characteristics were specified after separate analysis and experiments, shown in Table-1.

TABLE-1
CATALYST CHARACTERISTICS USED IN EXPERIMENTS

Weight percentage SiO_2	95.1
Weight percentage F_2O_3	4.9
Appearance density	1.1 g/cc
Granule porosity	0.61
Total surface (BET method)	360-370 m^2/g

The bed length in each experiment was more than 15 centimeters. Applied equipment schematic has been shown in Fig. 1. Reactants were drawn in cylinder and reservoir in Fig. 1. A pressure reducer, adjust the internal reactor pressure. Cylindrical reactor, warmed up with an electrical element to prevent the flash variation of temperature, also protects the catalytic bed at the reaction temperature. Sampling performs from products, with the analysis vessel, *via* a bypass adjacent to reactor.

Measurements: Firstly, air was fed into the reactor with about 50-250 cc/sec, then the reactor and catalysts warm up to reaction temperature of 180-210 °C. In order to turn on the electrical elements and adjust the consumption power catalysts warm up by 5 °C/min rate. After 50 min, the temperature of the catalyst bed will be fixed. Then, the H_2S gas valve will be opened, based on entering airflow, for the proper inlet flow, until the inlet concentration of H_2S gas remains fixed throughout the experiment. Outlet gases also sampling in a separately specific vessel and separate with elective absorption method and the concentration of each component was determined by iodometry method.
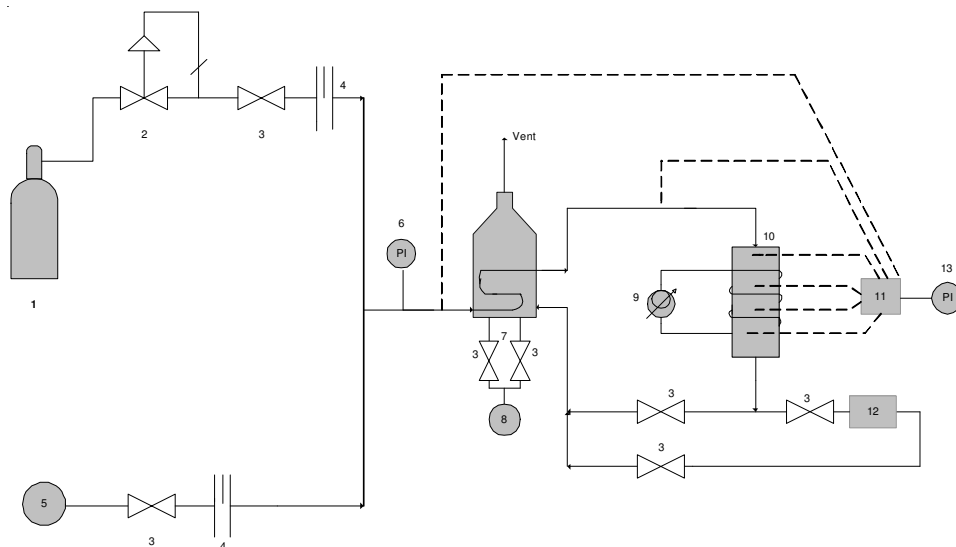
Fig. 1. Flow scheme of the equipment used. **1**, H$_2$S gas cylinder; **2**, adjustment regulator for outlet H$_2$S gas pressure; **3**, connection and disconnection gas valve; **4**, orifice; **5**, air reservoir; **6**, gauge; **7**, warmer of feed and burning the reactor outlet gases; **8**, mazote; **9**, adaptor of voltage and power for electrical warmer; **10**, thermocouple selecting key; **11**, fixed bed reactor; **12**, collection vessel of the outlet samples from reactor; **13**, gauge thermometer display

RESULTS AND DISCUSSION

To determine the rate relationship, the reaction conditions were so chosen to approximate the filmic and pores diffusion resistances to their minimum values, so the effects of these resistances minimize from rate relationship. As can be seen in eqn. 1 for the insignificant pores resistance.

$$\frac{[(-r')_{obs}][L^2]}{D_{eff}C_g} < 1 \tag{1}$$

Also, eqn. 2 for the slight filmic resistance:

$$\frac{\Phi D_{eff}}{K_g L} < 0.05 \tag{2}$$

The values has been obtained *via* performed measurements for the eqns. 1 and 2, are 0.3 and 0.0005, respectively. It can be concluded that the appeared reaction rate will be similar to real rate. Reaction rate values based on experimental measurements of reaction mixture components concentration are shown in Tables 2 and 3.

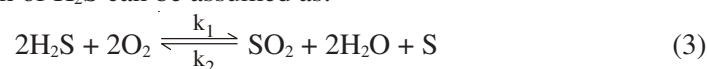Oxidation reaction of H$_2$S can be assumed as:

$$2H_2S + 2O_2 \underset{k_2}{\overset{k_1}{\rightleftharpoons}} SO_2 + 2H_2O + S \tag{3}$$

TABLE-2
OUTLET CONCENTRATION AND H_2S CONVERSION RATE AT 500 K

conc.	Run						
	1	2	3	4	5	6	7
C_{H_2S}	1.388×10^{-1}	1.530×10^{-1}	1.262×10^{-1}	1.711×10^{-1}	1.734×10^{-1}	1.660×10^{-1}	1.559×10^{-1}
C_{O_2}	4.316	4.312	4.363	4.363	4.371	4.372	4.354
C_{SO_2}	3.307×10^{-2}	3.825×10^{-2}	2.932×10^{-2}	4.602×10^{-3}	5.626×10^{-3}	4.036×10^{-3}	1.620×10^{-2}
C_{S_2}	1.386×10^{-4}	1.363×10^{-4}	1.496×10^{-4}	1.350×10^{-4}	1.316×10^{-4}	1.366×10^{-4}	1.373×10^{-4}
C_{S_6}	8.499×10^{-3}	8.359×10^{-3}	9.169×10^{-3}	8.276×10^{-3}	8.070×10^{-3}	8.372×10^{-3}	8.421×10^{-3}
C_{S_8}	2.298×10^{-2}	2.261×10^{-2}	2.480×10^{-2}	2.238×10^{-2}	2.182×10^{-2}	2.265×10^{-2}	2.4877×10^{-2}
C_{H_2O}	2.240×10^{-1}	3.063×10^{-1}	2.615×10^{-1}	2.289×10^{-1}	2.289×10^{-1}	2.358×10^{-1}	2.491×10^{-1}
$-r_{H_2S}$ (gmol/ gcat s)	7.400×10^{-8}	7.376×10^{-8}	7.443×10^{-8}	1.302×10^{-7}	1.281×10^{-7}	1.291×10^{-7}	1.010×10^{-7}

TABLE-3
OUTLET CONCENTRATION AND H_2S CONVERSION RATE AT 570 K

conc.	Run						
	1	2	3	4	5	6	7
C_{H_2S}	1.421×10^{-1}	5.465×10^{-1}	1.063×10^{-1}	7.977×10^{-2}	7.375×10^{-2}	3.995×10^{-2}	4.738×10^{-2}
C_{O_2}	3.678	3.722	3.696	3.720	3.713	3.746	3.727
C_{SO_2}	1.563×10^{-2}	5.792×10^{-2}	1.029×10^{-1}	8.147×10^{-3}	7.666×10^{-2}	4.140×10^{-2}	5.010×10^{-2}
C_{S_2}	7.799×10^{-5}	2.897×10^{-4}	1.826×10^{-4}	2.388×10^{-4}	2.492×10^{-2}	3.284×10^{-4}	2.731×10^{-5}
C_{S_6}	3.385×10^{-3}	1.258×10^{-3}	7.929×10^{-3}	1.015×10^{-2}	1.082×10^{-2}	1.425×10^{-2}	1.340×10^{-2}
C_{S_8}	5.91×10^{-3}	2.196×10^{-2}	1.384×10^{-2}	1.772×10^{-2}	1.888×10^{-2}	2.488×10^{-2}	2.368×10^{-2}
C_{H_2O}	2.240×10^{-1}	3.063×10^{-1}	2.615×10^{-1}	2.845×10^{-1}	2.931×10^{-1}	3.266×10^{-1}	3.200×10^{-1}
$-r_{H_2S}$ (gmol/ gcat s)	4.008×10^{-7}	1.625×10^{-7}	2.770×10^{-7}	2.766×10^{-7}	2.736×10^{-7}	1.299×10^{-7}	1.265×10^{-7}

Taking the above assumption, we can take the following relation rate for the H_2S conversion.

$$-r'_{H_2S} = k_1 C_{H_2S}^a C_{O_2}^b - k_2 C_S^c C_{SO_2}^d C_{H_2O}^e \tag{4}$$

However, the resulting values from experiments, which are given in the Tables 2 and 3, are not corresponding to this relation rate with little error. After computational consideration of experimental data in the various reaction pathways, extremely, an equation was concluded that can be in agreement with the experimental data values. This rate relation was produced with the assumption of two various reaction pathways for H_2S oxidation. These two reactions include:

$$H_2S + 1.5O_2 \xrightarrow{k_1} H_2O + SO_2 \tag{5}$$

$$2H_2S + SO_2 \underset{k_3}{\overset{k_2}{\rightleftharpoons}} 2H_2O + 3S \tag{6}$$
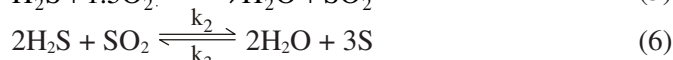
Obtained rate relation, which founded upon reaction pathways and produced results, explains so:

$$-r'_{H_2S} = k_1 C^a_{H_2S} + k_2 C^b_{H_2S} C^c_{SO_2} - k_3 C^d_S C^e_{H_2O} \qquad (7)$$

So the oxygen concentration is more than 10 times of H_2S all over the reactor length, therefore in equation 7 the oxygen concentration was neglected.

The calculated power and coefficient values from relation 7 at 500, 530 and 570 K are given in Table-4. These values were obtained by using the minimum square error method and the results produced from values of the Tables 2 and 3.

TABLE-4
RATE EQUATION COEFFICIENTS

Coefficient	T = 500 K	T = 530 K	T = 570 K
k_1	3.1570×10^{-7}	1.7301×10^{-6}	3.8598×10^{-6}
a	1.6364721	1.4901445	1.3650317
k_2	1.2206×10^{-7}	1.9234×10^{-7}	3.0022×10^{-7}
b	0.7194161	0.5712398	0.4407293
c	-0.2219540	-0.2071234	-0.199440
k_3	8.0529×10^{-11}	1.8976×10^{-9}	4.5801×10^{-8}
d	0.0000	0.0000	0.0000
e	0.0000	0.0000	0.0000

After determining the coefficient and powers ultimately, relation of H_2S conversion reaction rate can be written as:

$$-r'_{H_2S} = k_1 C^{3/2}_{H_2S} + k_2 C^{1/2}_{H_2S} C^{-1/5}_{SO_2} - k_3 \qquad (8)$$

$$k_i = \kappa_{o_i} \exp\left(\frac{-e_i}{Rt}\right) \qquad i = 1, 2, 3$$

$$\kappa_{o_i} = 216.8$$

E_i = 20.140 Kcal/mol K, $\kappa_{o_2} = 185.6 \times 10^{-6}$, E_2 = 7.312 Kcal/mol K, $\kappa_{o_3} = 1.6 \times 10^{12}$, E_3 = 50.66 Kcal/mol K.

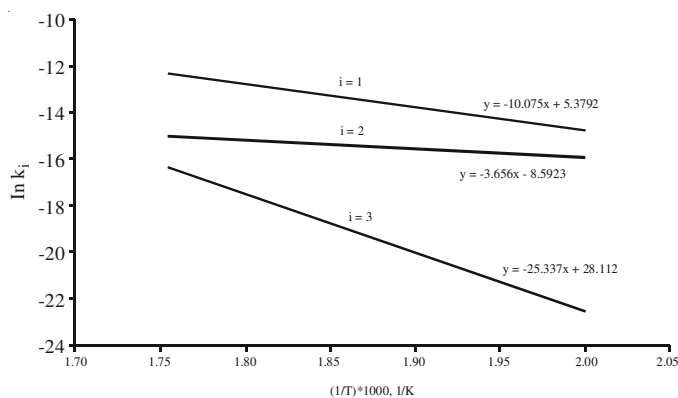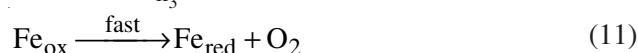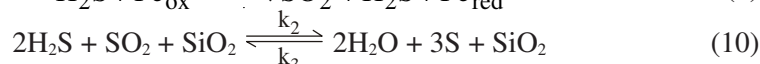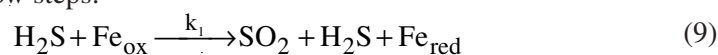Variation of rate coefficient logarithm *versus* temperature is shown in Fig. 2.

Fig. 2. Effect of temperature on the rate constants

Mechanism: As noted earlier, the equation 8 is the only resulted rate relation which is in good agreement with the obtained experimental values concluded by the two various reaction pathway assumptions, according to equations 5 and 6.

Therefore, with the acceptance that the H_2S conversion occurs in the reactor according to the above relations, the mechanism of this conversion can be considered according to the below steps:

$$H_2S + Fe_{ox} \xrightarrow{k_1} SO_2 + H_2S + Fe_{red} \tag{9}$$

$$2H_2S + SO_2 + SiO_2 \underset{k_3}{\overset{k_2}{\rightleftharpoons}} 2H_2O + 3S + SiO_2 \tag{10}$$

$$Fe_{ox} \xrightarrow{fast} Fe_{red} + O_2 \tag{11}$$

where, Fe_{ox} is the H_2S oxidation functionality and SiO_2 is the catalyst basis.

Conclusion

In accordance with equations 5 and 6 for the H_2S oxidation reaction, the results are as follows: (i) H_2S is consumed in both reactions. (ii) Sulphur is produced only in equilibrium reaction 6 which is competed with reaction 5. (iii) Since the reaction 5 is irreversible, therefore, if the amount of oxygen has controlled, all of the H_2S can be convert to sulphur. Considering these notes, we can describe the catalyst yield for the sulphur production in the following form:

$$\varphi = \frac{r'_S}{r'_{H_2S}} = \frac{k_2 C_{H_2S}^{3/2} C_{SO_2}^{-1/5} - k_3}{k_1 C_{H_2S}^{3/2} + k_2 C_{H_2S}^{-1/2} - k_3} \tag{12}$$

With reversing the reaction 12, we have:

$$\varphi^{-1} = 1 + \frac{k_1 C_{H_2S}^{3/2}}{k_2 C_{H_2S}^{1/2} C_{SO_2}^{-1.5} - k_3} \tag{13}$$

The smaller amount of right expression of equation 13 led to the greater yield of sulphur production.

It can be adjusted to the reactor conditions so the k_1 would be small as possible. In this situation, the progress degree of reaction 5, which produces SO_2, reaches the minimum level and after its production in this reaction, convert immediately to sulphur by reaction 6.

Temperature reduction is one of the several methods for reduction of k_1 and can increase the sulphur yield for the two reasons that consist of: (A) Reducing the temperature decreases the reaction progress rate 5. (B) The degree of sulphur production increases continuously with decreasing the temperature, according to calculated from values of thermodynamically equilibrium of the reaction 6.

The sulphur will be condensed and the catalyst pores will be gripped and causes to extensive decreases very much. Also according to equation 13, for increasing the yield of sulphur production, it should be equal to the SO_2 concentration relative to H_2S in its stociometric ratio in relation 6. For this aim, it is assumed that the H_2S enters from some area throughout the reactor.

Nomenclatures: a, b, c, d, e: Reaction rate degree

C_i: i component concentration in gas phase (gmol/m^3)

D_{eff}: Effective diffusion coefficient (m$_2$/s)

κ_i: Frequency factor   E: Activation energy (Kcal/mol.K)

κ_i: i component rate constant K_g: Gas phas mass transfer coefficient

L: Length characteristic of particle (m)

r'_i: Reaction rate of component i r'_{obs}: Observed rate of i component

T: Temperature (K) ϕ: Reaction yield

Φ: Thiele module

ACKNOWLEDGEMENT

REFERENCES

1. E. Laperdrix, A. Sahibed-dine, G. Costentin, M. Bensitel, J.C. Lavalley, *Appl. Catal. B Environ.*, **27**, 137 (2000).
2. H. Baehr, *Refiner Natl. Gas. Manuf.*, **17**, 237 (1938).
3. B.K. Kim, B.H. Hwang, H.S. Lee, H.C. Woo and D.W. Park, *Korean. J. Chem. Eng.*, **21**, 104 (2004).
4. B.G. Kim, W.D. Ju, I. Kim, H.C. Woo and D.W. Park, *Solid State Ionics*, **172**, 135 (2004).
5. M.Y. Shin, Ph.D. Thesis, Pohang University of Science and Technology (2000).
6. J.K. Chen and M.A. Huffmaster, Patent 7351392, to Shell Oil Company (2005).
7. B.G. Goar, *Oil Gas J.*, **25**, 96 (1975).
8. R. Kettner and N. Liermann, *Oil Gas J.*, **11**, 63 (1983).
9. R. Kettner, T. Lubcke and N. Liermann, Europe Patent 0078690, to Mobil Oil Corporation (1983).
10. P.J. Brink, J.W. Geus, Europe Patent 0409353, to VEG-Gasinstituut N.V. and Comprimo B.V. (1991).
11. P.J. van den Brink, R.J.A.M. Terorde, J.H. Moors, A.J. van Dillen and J.W. Geus, in: P. Ruiz, B. Delmon (Eds.), New Developments in Selective Oxidation by Heterogeneous Catalysis, Elsevier, Amsterdam, p. 123 (1991).
12. R.J.A.M. Terorde, P.J. van den Brink, L.M. Visser, A.J. van Dillen, *Catal. Today*, **17**, 217 (1993).
13. J.A. Lagas, J. Borsboom and P.H. Berben, *Oil Gas J.*, **86**, 68 (1988).
14. P.J. van den Brink, A. Scholten, A.J. van Dillen and J.W. Geus, in eds: C.H. Bartholomew, J.B. Butt, Catalyst Deactivation, Elsevier, Amsterdam, p. 515 (1991).
15. P.J. van den Brink, A. Scholten, A. van Wagenningen, M.D.A. Lamers, A.J. van Dillen and J.W. Geus, in eds.: G. Poncelet, P.A. Jacobs, P. Grange and B. Delmon, Preparation of Catalysts, Elsevier, Amsterdam, p. 527 (1991).
16. P.F.M.T. van Nisselrooy and J.A. Lagas, *Catal. Today*, **16**, 263 (1993).
17. E. Nasato, R.S. MacDougall and J.A. Lagas, *Oil Gas J.*, **28**, 45 (1994).
18. R.J.A.M. Terorde, M.C. de Jong, M.J.D. Crombag, P.J. Van den Brink, A.J. Van Dillen and J.W. Geus, *Stud. Surf. Sci. Catal.*, **82**, 861 (1994).
19. V.I. Marshneva and V.V. Mokrinskii, *Kinetics Catal.*, **29**, 989 (1988).
20. K.T. Li and N.S. Shyu, *Ind. Eng. Chem. Res.*, **36**, 1480 (1997).
21. K.T. Li, M.Y. Hyang and W.D. Cheng, US Patent 5653953 to Tunghai University (1997).
22. A. Sugier, P. Courty, A. Deschamps and H. Gruhier, US Patent 4197277, to Institut Prancais du Petrole (1980).